

# UC Irvine

## UC Irvine Previously Published Works

### Title

Removal of a mirror image and enhancement of the signal-to-noise ratio in Fourier-domain optical coherence tomography using an electro-optic phase modulator.

### Permalink

<https://escholarship.org/uc/item/5b62b9pm>

### Journal

Optics Letters, 30(2)

### ISSN

0146-9592

### Authors

Zhang, Jun  
Nelson, J Stuart  
Chen, Zhongping

### Publication Date

2005-01-15

### DOI

10.1364/ol.30.000147

### Copyright Information

This work is made available under the terms of a Creative Commons Attribution License, available at <https://creativecommons.org/licenses/by/4.0/>

Peer reviewed

# Removal of a mirror image and enhancement of the signal-to-noise ratio in Fourier-domain optical coherence tomography using an electro-optic phase modulator

Jun Zhang, J. Stuart Nelson, and Zhongping Chen

Beckman Laser Institute and the Center for Biomedical Engineering, University of California, Irvine, Irvine, California 92612

Received June 14, 2004

A novel swept-laser-based Fourier-domain optical coherence tomography system using an electro-optic phase modulator was demonstrated. The imaging range was doubled by cancellation of the mirror image. The elimination of low-frequency noises resulting from dc and autocorrelation terms increased the sensitivity by 20 dB. © 2005 Optical Society of America  
OCIS codes: 110.4500, 070.2590, 170.3880.

Optical coherence tomography (OCT) is a noninvasive, noncontact imaging modality that can provide micrometer-scale cross-sectional images of tissue microstructure.<sup>1</sup> Conventional OCT, which is based on a scanning optical delay line, is defined as time-domain OCT. An alternative OCT technique, i.e., Fourier-domain OCT (FDOCT), recently attracted much attention because of its potential for higher sensitivity and elimination of depth scanning.<sup>2-7</sup> However, dc and autocorrelation noise decrease the system sensitivity,<sup>4</sup> and the mirror image that is due to the Fourier transform limits the imaging range of FDOCT.<sup>8</sup> Several methods have been developed to resolve these problems. Phase retrieval algorithms using five interferograms with defined phase relations<sup>8</sup> or a 90° phase shift introduced by translation of the reference mirror<sup>9</sup> were adopted to obtain complex signals to cancel out the autocorrelation noise terms as well as the dc signal. However, these noninstantaneous algorithms require high stability of the systems and limit the imaging speed because of mechanical translation. The phase shift of an  $N$  by  $N$  ( $N > 2$ ) fiber coupler has been proposed as a means of access to the complex image, but this approach has the drawback of phase drift resulting from the temperature sensitivity of the coupler splitting ratio.<sup>10</sup> In this Letter a synchronous method using an electro-optic (EO) phase modulator in a swept-laser-based FDOCT system is demonstrated that can achieve a full-range complex signal to eliminate dc and autocorrelation noises as well as the mirror image.

In a FDOCT system the detected intensity can be expressed as

$$\begin{aligned}
 I(k) = & S(k)R_R + S(k) \int_{-\infty}^{+\infty} \int_{-\infty}^{+\infty} [R_S(\Delta z)R_S(\Delta z')]^{1/2} \\
 & \times \exp\{i[k(\Delta z - \Delta z') + \phi(\Delta z) - \phi(\Delta z')]\}d\Delta z d\Delta z' \\
 & + 2S(k)\sqrt{R_R} \int_{-\infty}^{\infty} \sqrt{R_S(\Delta z)} \cos[k\Delta z + \phi(\Delta z)]d\Delta z,
 \end{aligned} \tag{1}$$

where  $k$  is the wave number;  $S(k)$  is the spectral density of the laser source;  $R_R$  and  $R_S$  are the reflectivities of the reference and the sample arms, respectively;  $\Delta z$  and  $\Delta z'$  denote the double-pass path-length differences between the sample and the reference arms; and  $\phi$  is the phase shift. The first term in Eq. (1) represents the reflected intensity from the reference mirror. The second autocorrelation term is the mutual interference of all elementary waves in the sample under study. These two terms yield the dc and low-frequency noises that obscure the structure of the tissue under study. From the last interference term in Eq. (1), the depth information of the sample can be obtained by a Fourier transform from  $k$  to  $z$  space. Since the Fourier transform of a real function is Hermitian, the structure term is always accompanied by a mirror image. This can be illustrated by the Fourier transform of a simple sinusoidal interference term<sup>9</sup>:

$$\cos(k\Delta z) \xrightarrow{\text{FT}} \frac{1}{2} [\delta(z - \Delta z) + \delta(z + \Delta z)]. \tag{2}$$

In the case of a swept-laser-based FDOCT system, where the wave number  $k$  is a function of time,  $k = k(t)$ , the fringe signal can also be converted from time to frequency space by a Fourier transform. Because the maximum depth range of OCT imaging is limited by the strong attenuation of light with depth in tissue, the corresponding frequency functions of the interference and autocorrelation terms are also limited as long as the wave number is scanned smoothly. Thus, by choosing an appropriate carrier frequency, one can separate the negative and positive terms of the Fourier-transformed interference signal from each other. The low-frequency noise that resulted from dc and autocorrelation terms is not affected by the carrier frequency and can be separated from the interference signal. The needed carrier frequency can be estimated as a distance shift in  $z$  space. For simplicity, a linearly swept laser source, i.e.,  $k = k_0 - mt$ , was adapted for the estimation. The sinusoidal interference term can be written as

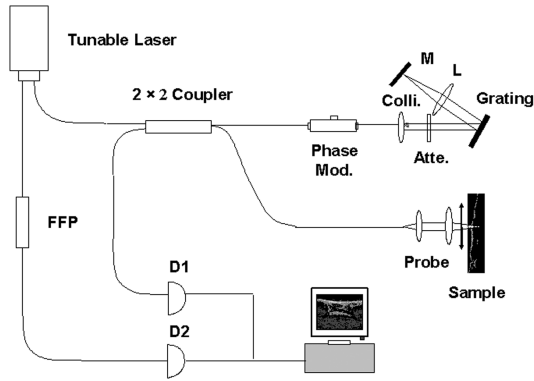


Fig. 1. Schematic of the FDOCT system. Phase Mod., phase modulator; Colli., collimator; Atte., adjustable neutral-density attenuator; M, mirror; L, lens; FFP, 100-GHz fiber Fabry-Perot interferometer; D1, D2, photodetectors.

$$\begin{aligned}
 \cos(k\Delta z - \Omega t) &= \cos\left[k\left(\Delta z + \frac{\Omega}{m}\right) - \frac{\Omega k_0}{m}\right] \\
 &= \cos\left[k(\Delta z + z_0) - \frac{\Omega k_0}{m}\right] \\
 \xrightarrow{\text{FT}} \frac{1}{2} &\left[\delta(z - \Delta z - z_0)\exp\left(i\frac{\Omega k_0}{m}\right) + \delta(z + \Delta z + z_0)\exp\left(-i\frac{\Omega k_0}{m}\right)\right], \quad (3)
 \end{aligned}$$

where  $\Omega$  is the angular carrier frequency and  $z_0 = \Omega/m$  is the corresponding double-pass distance shift. Compared with expression (2), the negative and positive terms of the Fourier-transformed interference signal are separated by a generated distance of  $2z_0$ . Therefore the image can be constructed from only the positive (or negative) term.

A schematic diagram of the fiber-based FDOCT system is shown in Fig. 1. The output light from a swept laser source (Micron Optics) at  $1.31 \mu\text{m}$  with a FWHM bandwidth of 85 nm and an output power of 5 mW is split into reference and sample arms by a  $2 \times 2$  coupler. The laser source was driven by a 500-Hz sinusoidal signal. The effective sweep time through the total tuning range of 120 nm is 0.68 ms. In the reference arm an EO phase modulator (JDS Uniphase) was used to generate a stable carrier frequency of 500 kHz. According to expression (3) the corresponding double-pass distance shift is  $\sim 5$  mm, which is sufficient to separate the positive and negative terms as well as the low-frequency terms. To match dispersion caused by the EO phase modulator, an optical setup similar to a rapid-scanning optical delay line<sup>11</sup> with a stationary mirror was adopted that can compensate for group-velocity dispersion. Calculation showed that the higher-order dispersion can be neglected in our system. Nevertheless, for ultrahigh-resolution FDOCT systems, it is necessary to take into account the higher-order dispersion, which can be canceled by software-based dispersion-compensation methods.<sup>12,13</sup> The reference power was

attenuated by an adjustable neutral-density attenuator for maximum sensitivity.<sup>14</sup> We split 5% of the laser output and propagated it through a 100-GHz fiber Fabry-Perot interferometer (Micron Optics) to generate comb signals for dynamic calibration of the swept spectra, which is essential for rigorous conversion from time to wave-number space. In the detection arm the signal from the photodetectors was converted by 12-bit data acquisition board sampling at 10 MHz, and the number of data points for each A-line data acquisition was 5000. The complex analytical depth-encoded signal  $\tilde{S}(z)$  was converted from time fringe signal  $\Gamma(t)$  by the digital approach shown in Fig. 2, where FFT denotes the fast Fourier transform,  $\times$  is a multiplication symbol,  $H(v)$  is the Heaviside function given by

$$H(v) = \begin{cases} 0 & v < 0 \\ 1 & v \geq 0 \end{cases}, \quad (4)$$

and  $\text{FFT}^{-1}$  denotes the inverse fast Fourier transform. Time fringe signal  $\Gamma(t)$  is first transformed from time to frequency space by a fast Fourier transform. Multiplication of the Heaviside function and the process

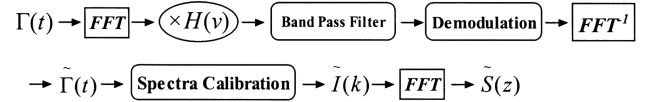
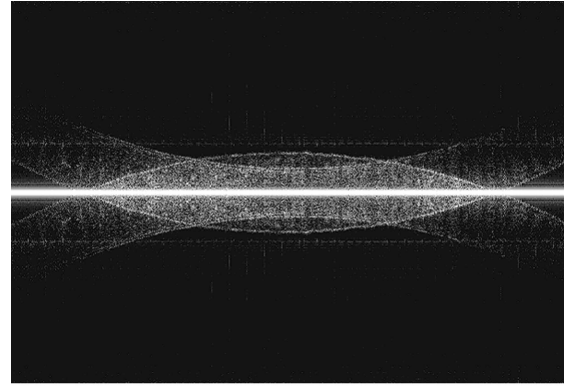
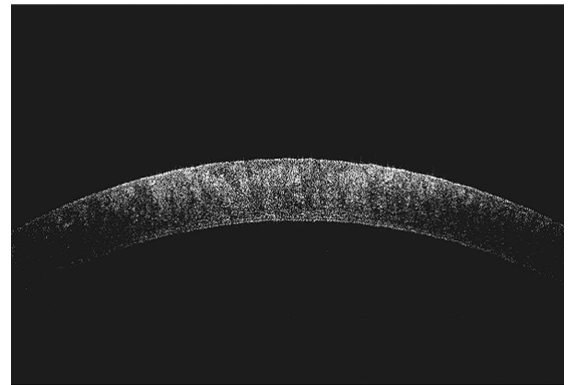


Fig. 2. Block diagram of conversion from time fringe signal  $\Gamma(t)$  to complex analytical depth-encoded signal  $\tilde{S}(z)$ .



(a)



(b)

Fig. 3. Images of rabbit cornea obtained with the FDOCT system (a) without and (b) with an EO phase modulator.

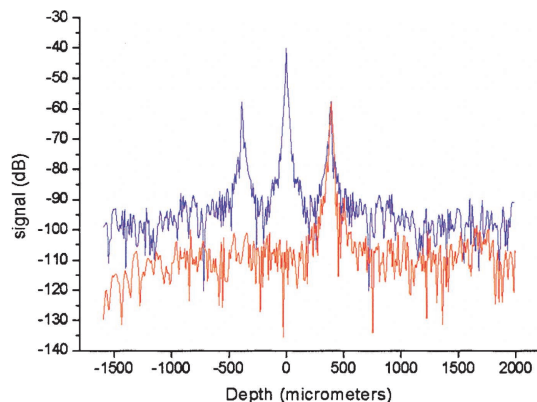


Fig. 4. Sensitivities measured with a  $-57.6$ -dB reflector. Blue, without an EO phase modulator; red, with an EO phase modulator.

of bandpass filtering are used to select the positive term of the Fourier-transformed interference signal. The subsequent demodulation step removes the carrier frequency and is critical for the cancellation of distortion that is due to the nonlinearities in the wave-number scan. The frequency fringe signal is then converted back to time space by  $\text{FFT}^{-1}$ . The spectra calibration determines the function of  $k(t)$  before conversion from time to wave-number space. The complex depth-encoded fringe signal  $\tilde{S}(z)$  was finally obtained by Fourier transform from  $k$  to  $z$  space. From the amplitude information of  $\tilde{S}(z)$ , the structure image can be acquired. To illustrate the performance of the system, a rabbit cornea was imaged as shown in Fig. 3. The imaged area is  $6 \text{ mm} \times 4.1 \text{ mm}$  with the zero distance difference set in the center of the depth scale. Compared with the image obtained by a conventional FDOCT system without an EO phase modulator, the overlapped mirror images and autocorrelation noise close to the zero position were eliminated by our novel FDOCT system. The system sensitivity was measured with a  $-57.6$ -dB partial reflector that was placed  $390 \mu\text{m}$  from the zero position. A sensitivity improvement of 20 dB was obtained, as shown in Fig. 3.

In summary, a novel swept-laser-based FDOCT system using an EO phase modulator has been demonstrated. The imaging range was doubled by removal of the mirror image. The sensitivity measurement

showed a 20-dB increase in signal-to-noise ratio by the elimination of low-frequency noises due to dc and autocorrelation terms.

This work was supported by research grants awarded from the National Science Foundation (BES-86924), National Institutes of Health (EB-00293, EB-00255 and EB-002495, NCI-91717, and RR-01192), the U.S. Air Force Office of Scientific Research (F49620-00-1-0371), and the Beckman Laser Institute Endowment. Loan of the  $1.31\text{-}\mu\text{m}$  swept source from Micron Optics, Inc., and discussions with Keven Hsu are also gratefully acknowledged. Z. Chen's e-mail address is zchen@bli.uci.edu.

## References

1. D. Huang, E. A. Swanson, C. P. Lin, J. S. Schuman, W. G. Stinson, W. Chang, M. R. Hee, T. Flotte, K. Gregory, C. A. Puliafito, and J. G. Fujimoto, *Science* **254**, 1178 (1991).
2. A. F. Fercher, C. K. Hitzenberger, G. Kamp, and S. Y. El-Zaiat, *Opt. Commun.* **117**, 43 (1995).
3. G. Hausler and M. W. Lindner, *J. Biomed. Opt.* **3**, 21 (1998).
4. R. Leitgeb, C. K. Hitzenberger, and A. F. Fercher, *Opt. Express* **11**, 889 (2003), <http://www.opticsexpress.org>.
5. J. F. de Boer, B. Cense, B. H. Park, M. C. Pierce, G. J. Tearney, and B. E. Bouma, *Opt. Lett.* **28**, 2067 (2003).
6. M. A. Choma, M. V. Sarunic, C. H. Yang, and J. A. Izatt, *Opt. Express* **11**, 2183 (2003), <http://www.opticsexpress.org>.
7. S. H. Yun, G. J. Tearney, J. F. de Boer, N. Iftimia, and B. E. Bouma, *Opt. Express* **11**, 2953 (2003).
8. M. Wojtkowski, A. Kowalczyk, R. Leitgeb, and A. F. Fercher, *Opt. Lett.* **27**, 1415 (2002).
9. R. A. Leitgeb, C. K. Hitzenberger, A. F. Fercher, and T. Bajraszewski, *Opt. Lett.* **28**, 2201 (2003).
10. M. A. Choma, C. Yang, and J. A. Izatt, *Opt. Lett.* **28**, 2162 (2003).
11. G. J. Tearney, B. E. Bouma, and J. G. Fujimoto, *Opt. Lett.* **22**, 1811 (1997).
12. M. Wojtkowski, V. J. Srinivasan, T. H. Ko, J. G. Fujimoto, A. Kowalczyk, and J. S. Duker, *Opt. Express* **12**, 2404 (2004), <http://www.opticsexpress.org>.
13. B. Cense, N. A. Nassif, T. C. Chen, M. C. Pierce, S. Yun, B. H. Park, B. E. Bouma, G. J. Tearney, and J. F. de Boer, *Opt. Express* **12**, 2435 (2004), <http://www.opticsexpress.org>.
14. W. V. Sorin and D. M. Baney, *IEEE Photon. Technol. Lett.* **4**, 1404 (1992).